Design Proposal: Mach–Zehnder Interferometer

Arefur Rahman

I. Introduction

Mach–Zehnder interferometers (MZIs) are fundamental building blocks in integrated photonics and are widely used for applications including optical filtering, modulation, switching, and sensing. Their spectral response is highly sensitive to phase differences between two optical paths, making them especially suitable for wavelength-selective devices and on-chip signal processing in silicon photonic platforms.

In this work, we investigate the design and modeling of unbalanced silicon photonic MZIs using compact waveguide models suitable for circuit-level simulation. Two interferometer implementations are considered: an MZI employing Y-branches for both splitting and recombination, and an MZI using a Y-branch splitter combined with a broadband directional coupler. The primary objective of this design proposal is to analyze how the interferometer architecture and differential path length influence the transfer function and free spectral range.

II. Theory

A. Transfer Function of a Mach–Zehnder Interferometer

The Mach–Zehnder interferometer (MZI) consists of an input optical signal that is split into two branches and subsequently recombined. The splitting and combining operations can be implemented using various optical components, including Y-branches and directional couplers. In this design proposal, we consider two interferometer implementations: (i) an MZI formed using two Y-branches and (ii) an MZI formed using a Y-branch as the splitter and a broadband directional coupler as the combiner.

Let the input optical intensity be I_i, corresponding to an input electric field E_i. At the output of the splitter, the field is equally divided between the two arms such that

$$E_1 = \frac{E_i}{\sqrt{2}}, \qquad E_2 = \frac{E_i}{\sqrt{2}}. \tag{1}$$

The propagation of light in the two waveguides is described by the propagation constants

$$\beta_1 = \frac{2\pi n_1}{\lambda}, \qquad \beta_2 = \frac{2\pi n_2}{\lambda}, \tag{2}$$

where n_1 and n_2 are the effective refractive indices of the two waveguides, and λ is the vacuum wavelength. The waveguide lengths are L_1 and $L_2 = L_1 + \Delta L$, with corresponding power attenuation coefficients α_1 and α_2.

At the inputs of the combiner, the optical fields are

$$E_{o1} = \frac{E_i}{\sqrt{2}} e^{-i\beta_1 L_1 - \frac{\alpha_1}{2} L_1}, \tag{3}$$

$$E_{o2} = \frac{E_i}{\sqrt{2}} e^{-i\beta_2 L_2 - \frac{\alpha_2}{2} L_2}. \tag{4}$$

Two Y-branch MZI: When the combiner is implemented using a second Y-branch, the output field is given by

$$E_o = \frac{1}{\sqrt{2}}(E_{o1} + E_{o2}) = \frac{E_i}{2}\left(e^{-i\phi_1} + e^{-i\phi_2}\right), \tag{5}$$

where $\phi_k = \beta_k L_k$. The corresponding output intensity is

$$I_o = \frac{I_i}{4}\left|e^{-i\phi_1} + e^{-i\phi_2}\right|^2. \tag{6}$$

Neglecting propagation loss ($\alpha_1 = \alpha_2 = 0$), this simplifies to the well-known MZI transfer function

$$I_o = \frac{I_i}{2}\left[1 + \cos(\phi_1 - \phi_2)\right]. \tag{7}$$

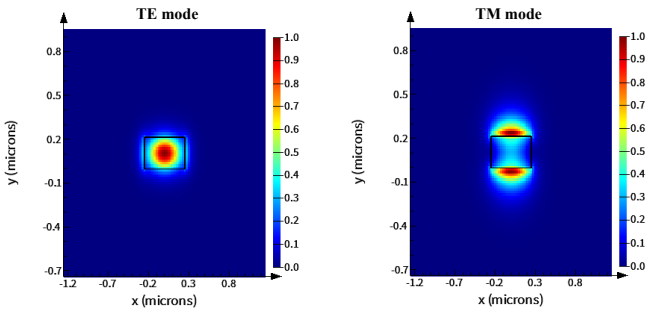

Fig. 1. Simulated mode profile.

Y-branch and directional-coupler MZI: If the output combiner is instead implemented using a broadband directional coupler, the recombination introduces an additional $\pi/2$ relative phase shift between the two inputs. For an ideal $50/50$ directional coupler, the output field can be written as

$$E_o = \frac{1}{\sqrt{2}}(E_{o1} + iE_{o2}) = \frac{E_i}{2}\left(e^{-i\phi_1} + ie^{-i\phi_2}\right). \tag{8}$$

The resulting output intensity is

$$I_o = \frac{I_i}{4}\left|e^{-i\phi_1} + ie^{-i\phi_2}\right|^2, \tag{9}$$

which, in the absence of loss, simplifies to

$$I_o = \frac{I_i}{2}\left[1 + \sin(\phi_1 - \phi_2)\right]. \tag{10}$$

Email: rahma221@purdue.edu

Thus, replacing the output Y-branch with a directional coupler introduces a constant $\pi/2$ phase offset in the interferometer response. Both implementations are equivalent up to this fixed phase bias and exhibit the same free spectral range, which is determined solely by the optical path-length difference ΔL.

B. Free Spectral Range of an Imbalanced Interferometer

Given the transfer function of an imbalanced Mach–Zehnder interferometer in 10, we seek to determine the spacing between adjacent transmission maxima, referred to as the free spectral range (FSR),

$$\mathrm{FSR} = \Delta\lambda = \lambda_{m+1} - \lambda_m. \tag{11}$$

The phase term in the interferometer transfer function is defined as

$$\delta = \beta \Delta L, \tag{12}$$

where the propagation constant is

$$\beta = \frac{2\pi n}{\lambda}, \tag{13}$$

with n denoting the effective refractive index and λ the vacuum wavelength. Adjacent transmission peaks correspond to a phase difference of 2π, such that

$$\Delta\delta = \delta_m - \delta_{m+1} = 2\pi. \tag{14}$$

In typical interferometers, many fringes are observed across the spectrum, implying operation at high interference order ($\delta \gg 2\pi$). Writing the phase difference explicitly in terms of the propagation constants at adjacent peaks yields

$$2\pi = \delta_m - \delta_{m+1} = \beta_m \Delta L - \beta_{m+1} \Delta L. \tag{15}$$

This gives the corresponding change in propagation constant,

$$\Delta\beta = \beta_m - \beta_{m+1} = \frac{2\pi}{\Delta L}. \tag{16}$$

Assuming that β varies approximately linearly with wavelength over the interval of interest, we write

$$\Delta\beta \approx -\frac{d\beta}{d\lambda}\Delta\lambda. \tag{17}$$

Combining the above expressions leads to

$$\Delta\lambda \approx -\frac{2\pi}{\Delta L}\left(\frac{d\beta}{d\lambda}\right)^{-1}. \tag{18}$$

To evaluate $d\beta/d\lambda$, we differentiate $\beta = 2\pi n/\lambda$ with respect to λ,

$$\frac{d\beta}{d\lambda} = \frac{2\pi}{\lambda}\frac{dn}{d\lambda} - \frac{2\pi n}{\lambda^2} = -\frac{2\pi}{\lambda^2}\left(n - \lambda\frac{dn}{d\lambda}\right). \tag{19}$$

Substituting this result into the expression for $\Delta\lambda$ yields the free spectral range,

$$\mathrm{FSR} = \Delta\lambda = \frac{\lambda^2}{\Delta L\left(n - \lambda\frac{dn}{d\lambda}\right)}. \tag{20}$$

Defining the group index n_g as

$$n_g = n - \lambda\frac{dn}{d\lambda}, \tag{21}$$

the free spectral range can be written in its commonly used form,

$$\mathrm{FSR} = \frac{\lambda^2}{\Delta L\, n_g}. \tag{22}$$

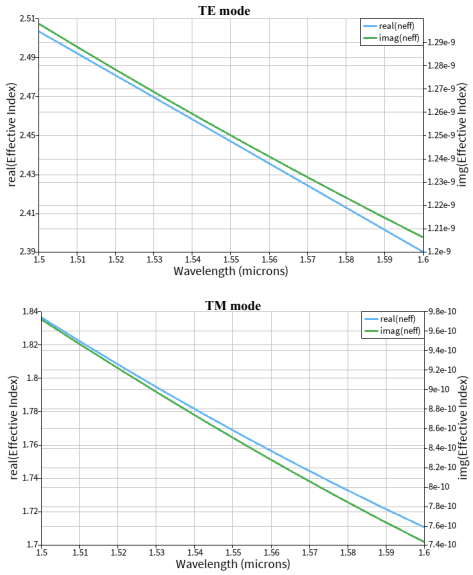

Fig. 2. Simulated fundamental modes effective index.

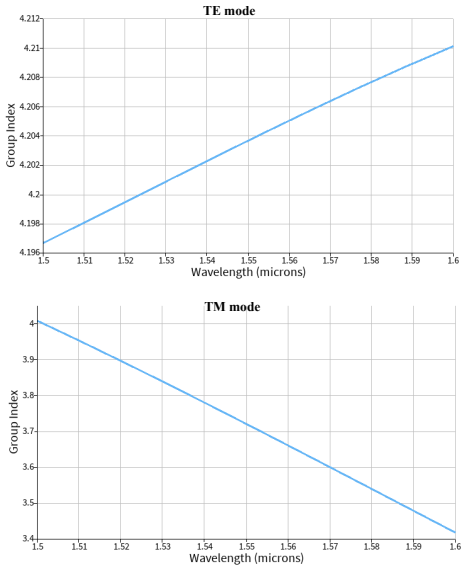

Fig. 3. Simulated fundamental modes group index.

TABLE I
COMPACT MODEL COEFFICIENTS

Coefficient	Value
n_1	2.43361
n_2	-1.13284
n_3	-0.394493

III. MODELLING AND SIMULATION

A. Waveguide

The optical waveguide was analyzed using the eigenmode solver in Lumerical MODE. The simulated structure consists of a silicon strip waveguide with a core thickness of 220 nm and a width of 500 nm, surrounded by a silicon dioxide cladding. At the design wavelength, the fundamental transverse-electric (TE) and transverse-magnetic (TM) modes were computed to verify single-mode operation.

To evaluate the dispersive properties of the waveguide, eigenmode simulations were performed over the wavelength range from 1500 nm to 1600 nm. From these simulations, the wavelength-dependent effective index $n_{\text{eff}}(\lambda)$ and group index $n_g(\lambda)$ were extracted.

For efficient circuit-level modeling, the simulated effective index was approximated using a compact analytical expression. Specifically, $n_{\text{eff}}(\lambda)$ was fitted to a second-order Taylor expansion about a reference wavelength λ_0,

$$n_{\text{eff}}(\lambda) = n_1 + n_2(\lambda - \lambda_0) + n_3(\lambda - \lambda_0)^2. \qquad (23)$$

The fitted coefficients n_1, n_2, and n_3 are summarized in Table II. This compact model closely reproduces the numerical eigenmode results over the wavelength range of interest and enables efficient simulation of interferometric circuits.

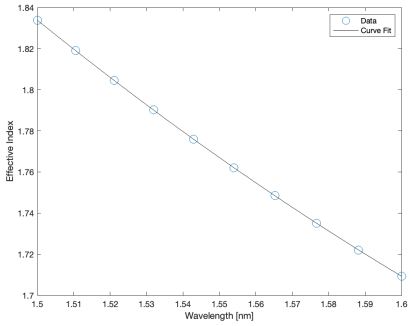

Fig. 4. Simulated compact model fitted effective index

B. MZI Circuit

The Mach–Zehnder interferometers were modeled and simulated using the EBeam compact models from the SiEPIC-EBeam-PDK within Lumerical INTERCONNECT. For an unbalanced MZI, the primary design parameter is the differential path length ΔL, which directly determines the free spectral range, as derived in the previous section.

To quantify this dependence, a set of MZIs with varying values of ΔL was simulated. The resulting free spectral ranges

TABLE II
EXPECTED FREE SPECTRAL RANGE FROM PATH-LENGTH DIFFERENCE

ΔL (nm)	FSR (nm)
50	11.7
102	5.6
102(RR)	2.5
265	2.16
270(TM)	2.4
602	0.96
650	0.9

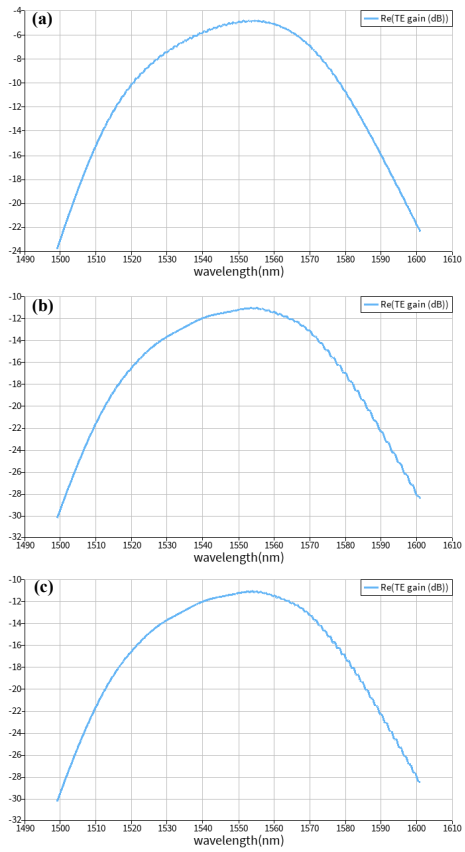

Fig. 5. Insertion loss reference spectrum of (a): grating coupler, (b),(c): y-branch splitter.

are summarized in Table II, where *RR* denotes an MZI circuit with a ring resonator embedded in one interferometer arm, and *TM* indicates operation in the transverse-magnetic waveguide mode. For a given path length difference, the inclusion of a ring resonator in one arm leads to a reduced FSR due to the increased effective optical path length. Each device was analyzed in the wavelength domain using spectral sweeps from 1500 nm to 1600 nm in INTERCONNECT.

The simulated responses include insertion loss contributions from the grating couplers (Fig. 5(a)), as well as from the combined grating couplers and Y-branch splitters (Fig. 5(b,c)). Transmission spectra were evaluated for both transverse-electric (TE) polarization (Fig. 6(a–c)) and transverse-magnetic (TM) polarization (Fig. 6(d)) for MZIs implemented using two Y-branches. Transmission responses were also simulated for MZIs employing a Y-branch splitter combined with a directional coupler at the output (Fig. 7(a,b)),

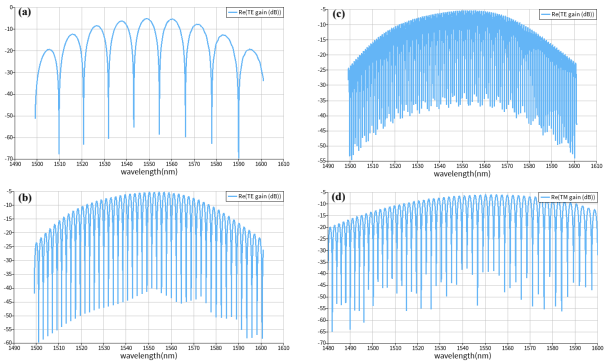

Fig. 6. (a),(b),(c): Y-branch splitter/combiner based MZI transmission for variable path length difference.

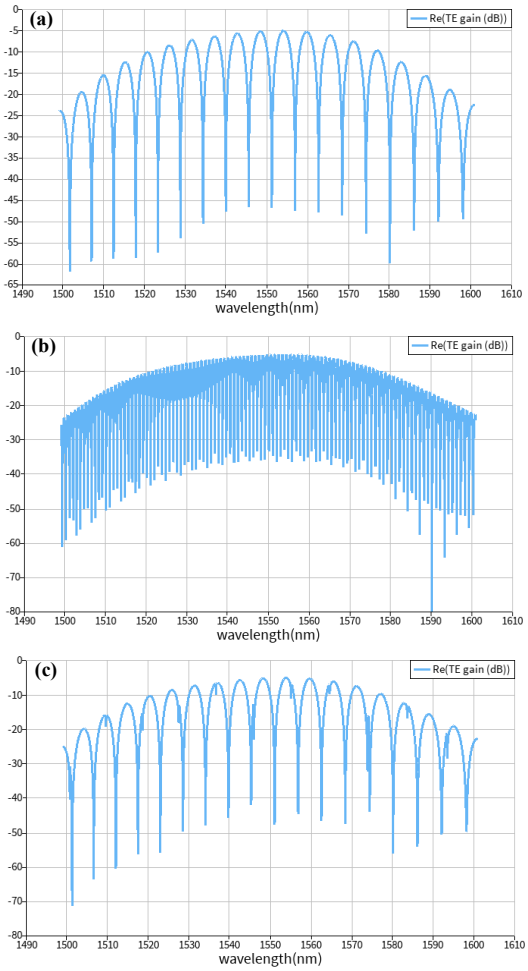

Fig. 7. (a),(b),(c): Y-splitter, broadband directional coupler, and ring resonator based MZI transmission.

as well as for a configuration incorporating a ring resonator in one interferometer arm (Fig. 7(c)).

REFERENCES

[1] L. Chrostowski and M. Hochberg, *Silicon Photonics Design*. Cambridge University Press, 2015.

[2] L. Chrostowski, et al. "Design and simulation of silicon photonic schematics and layouts." *Silicon Photonics and Photonic Integrated Circuits V* Vol. 9891. SPIE, 2016.